

RadExPro
seismic software

Diffraction imaging

(Revised 19.12.2023)

RADEXPRO EUROPE OÜ

Järvevana tee 9-40
11314 Tallinn, ESTONIA

RADEXPRO SEISMIC SOFTWARE LLC

29, Tornike Eristavi str.
Tbilisi, Georgia

t: +995 557 659 289

www.radepro.com

E-mails:

support@radepro.com

sales@radepro.com

Content

Content	2
Introduction.....	3
Diffraction separation	4
Diffraction imaging.....	5
Migration	5
Migration postprocessing	6
Semblance	7
N-th root migration.....	8
References.....	10

Introduction

*NB: This tutorial is intended for **RadExPro Professional/Real-Time** version 2023.4 and later.*

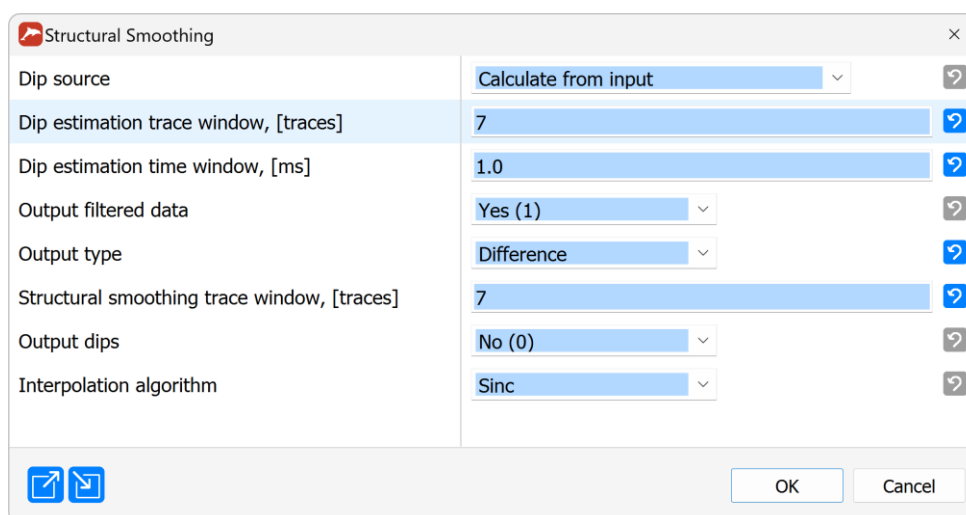
This tutorial is for the users who aim to apply **RadExPro** for the purposes of diffraction imaging. Diffraction imaging involves separating the diffractions from the reflected wavefield and analyzing them. The diffraction images can be used to study local heterogeneities in the subsurface, such as boulders, small gas pockets, and faults. The tutorial presents an example of a diffraction imaging workflow, which contains the diffraction separation with the **Structural Smoothing** module and the migration of diffractions/diffraction semblance computation with the **Pre/Post-Stack Kirchhoff Time Migration***, as well as the N-th root wavefield computation with **Power of Trace**, which can be useful for the detection of weak diffracted signals.

The tutorial is accompanied by a **RadExPro** project where the explained steps are present as processing flows.

Diffraction separation

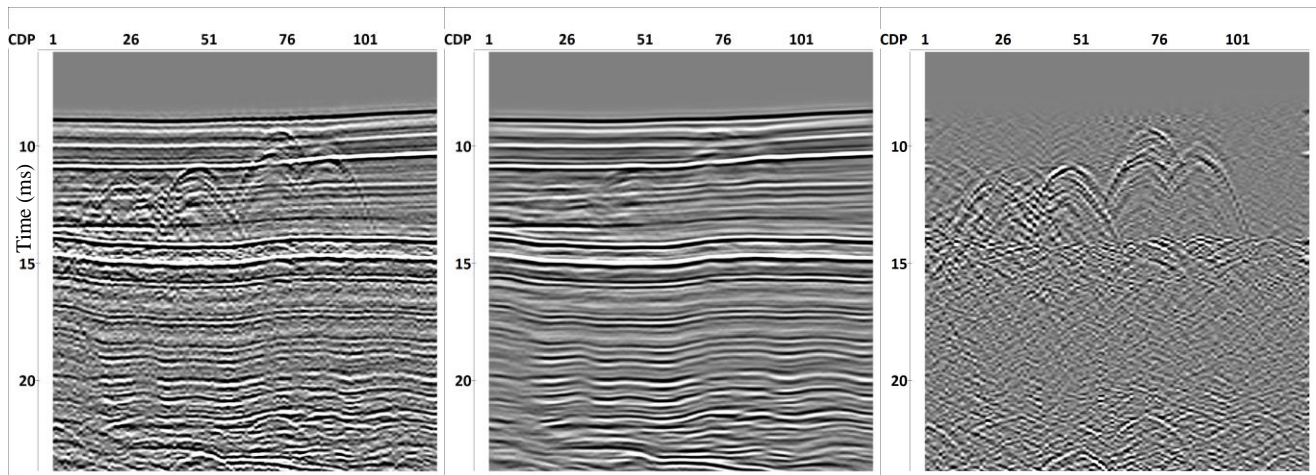
To enable diffraction imaging, one needs to separate the diffractions from the reflections in the recorded seismic wavefield. In **RadExPro**, this can be done with the **Structural Smoothing** module. This module estimates the dip of the event with the highest energy at every point in the seismic gather and smooths the data along this dip, e.g., Fomel (2002). The dips are estimated in sliding windows. In most cases, the reflections are the strongest events in the data, so the module will smooth the data along the reflections, thus attenuating the diffractions. Then, we can obtain the diffracted wavefield by subtracting the smoothing result from the input dataset.

We apply this method to a single-channel high-resolution seismic dataset. In the tutorial project, the diffraction separation occurs in the flow *002-diff-separation*. The suggested **Structural Smoothing** parameters for this dataset are shown in the Figure below.



Parameters of the Structural Smoothing module

Here, the main parameters which govern the effectiveness of the diffraction separation are the *Dip estimation trace window, [traces]*, *Dip estimation time window, [ms]* and *Structural smoothing trace window, [traces]*. The dip estimation window size needs to be large enough to contain enough reflection energy, but smaller than the characteristic sizes of the structures in the studied seismic section. Too large windows will lead to inaccurate dip estimation (the module can output the estimated dips for a detailed analysis). A similar behavior occurs for the *Structural smoothing trace window* parameter – using larger windows will lead to more effective reflection estimation and, thus, more effective diffraction separation, however, using the window size which is too large will lead to the leaking of reflections into the diffraction image. Note that the module contains a switch for subtracting the smoothing result from the input dataset – we use it here to obtain the diffractions with *Output type = Difference*. Also, we use *Interpolation algorithm = Sinc* for higher separation accuracy. The Figure below shows the input data, the smoothed reflections, and the separated diffractions.



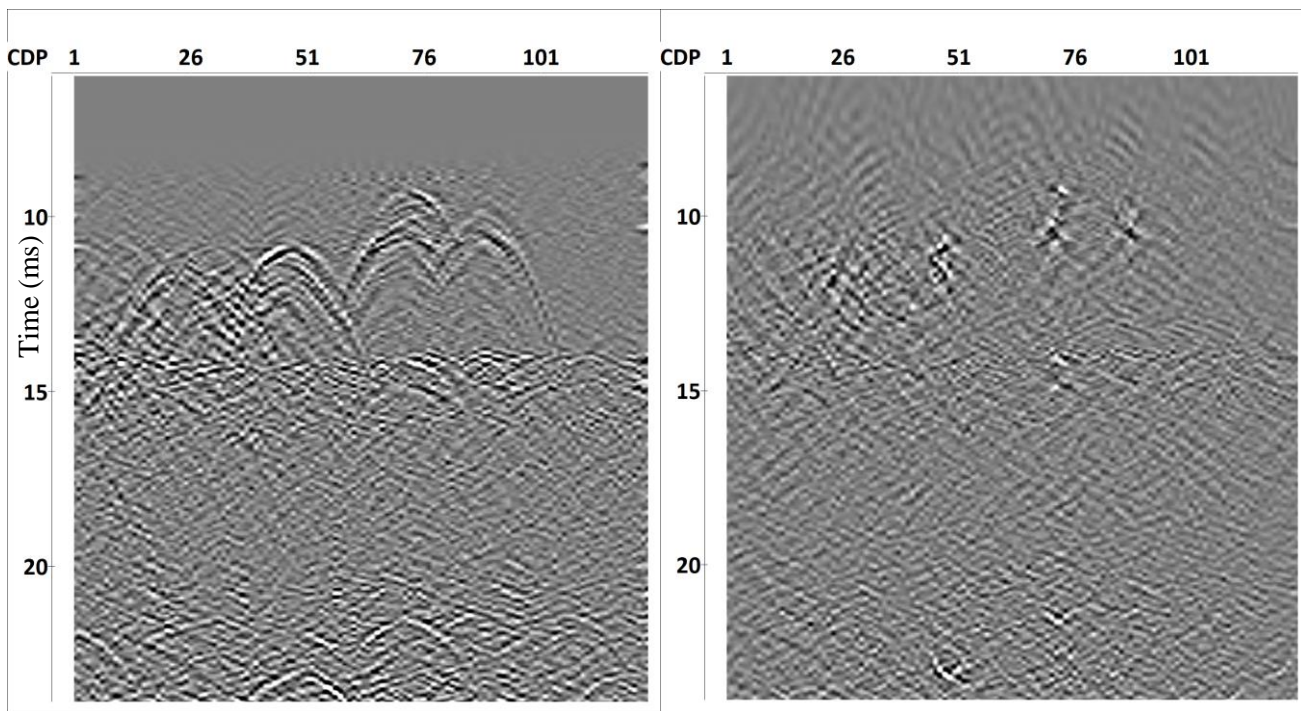
Input seismic data (left), smoothed reflections (center) and separated diffractions (right)

For 3D data, one can apply the smoothing algorithm first along the inline direction, and then along the crossline direction to obtain the reflections, which are then subtracted from the original cube to obtain the diffractions (sometimes, a single smoothing application in one direction can be enough). For pre-stack data, the same can be done on common-offset sections or common-offset cubes, although the separation might get more complex for long offsets, where the slopes of diffractions and reflections can get quite similar.

Diffraction imaging

Migration

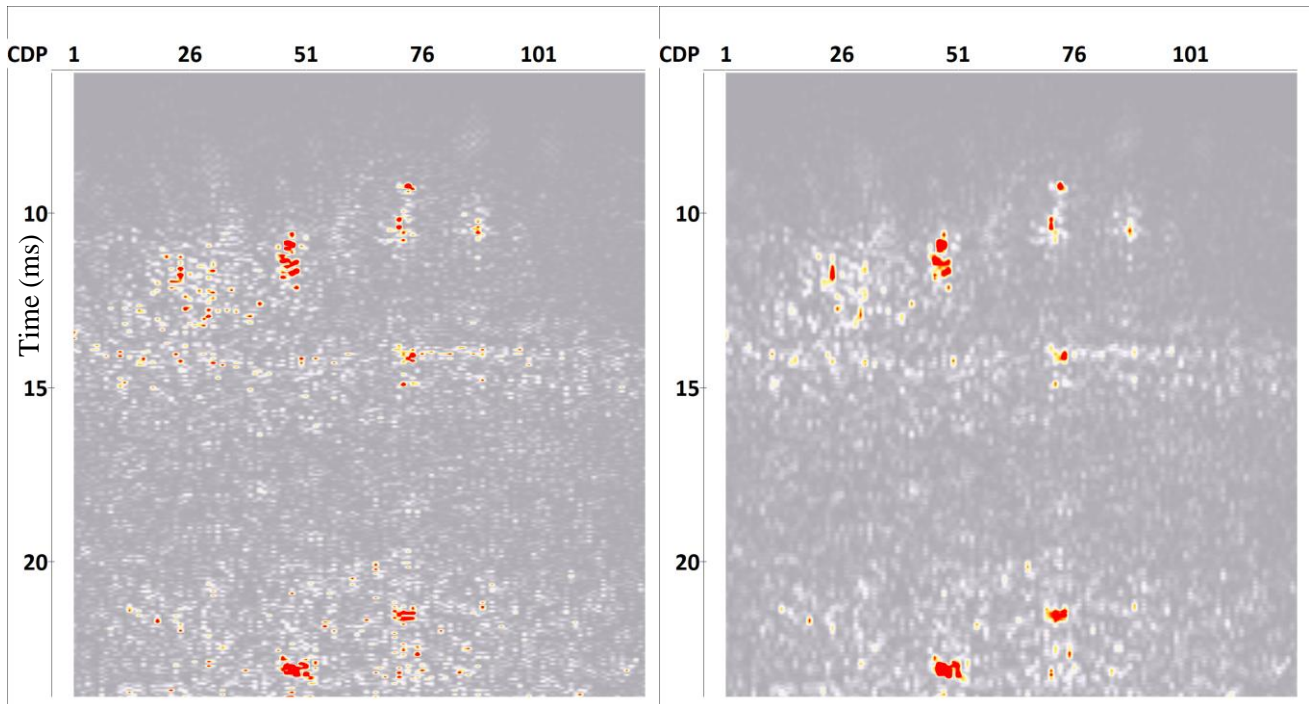
After the diffractions are separated from the reflections, one can analyze their hyperbolic traveltimes to get an estimate of subsurface velocity (Decker et al., 2017). We, however, assume that the velocity is already known from the conventional seismic processing, so the next step is migrating the diffractions. The migration occurs in the flow *003-migration*. We migrate the diffracted wavefield using the [Pre/Post-Stack Kirchhoff Time Migration*](#) module (other migration modules in **RadExPro** can also be used for this purpose). The module is set up like one would normally set up the seismic migration, with one small difference. Here, we choose not to apply the migration shaping filter. The shaping filter aims at preserving the reflected waveforms after migration. In our case, only the diffracted waves are migrated, which do not require a shaping filter (Denisov, 2017). Turning the shaping filter off allows us to expect symmetric diffraction waveforms in the migration result centered on the anomaly, assuming the input data is zero-phase, and the anomaly is a local heterogeneity like a boulder, for example. The migration result is compared to the original diffracted wavefield in the Figure below.



Diffracted wavefield before and after migration

Migration postprocessing

After computing the migration, we can analyze the wavefield as is. However, for tasks such as boulder detection, it is convenient to analyze the diffraction energy attribute. We compute the diffraction energy in the flow *004-postprocessing* by applying the [Power of Trace](#) module to the migration result with *Power exponent* equal to 2 with *Keep sign* turned off. Theoretically, one could choose ‘*Positive only*’ or ‘*Negative only*’ mode in the [Power of Trace](#) module to analyze only the diffracted anomalies of the specified sign. This attribute can then be optionally smoothed with the [2D Spatial Filtering](#) for display purposes. One can observe the original and smoothed diffraction energy in the Figures below. The diffraction energy maxima are aligned with the diffraction hyperbola apexes in the original seismic data, which means that this attribute can be applied for tasks such as boulder detection.



Diffraction energy computed without (left) and with (right) smoothing

Semblance

The diffraction energy shown above can be good enough for diffraction analysis. However, there is another attribute which can be computed from diffracted wavefield. This attribute is the diffraction semblance (Schwarz, 2019). The diffraction semblance S at a space-time location x_0, t_0 is computed as follows:

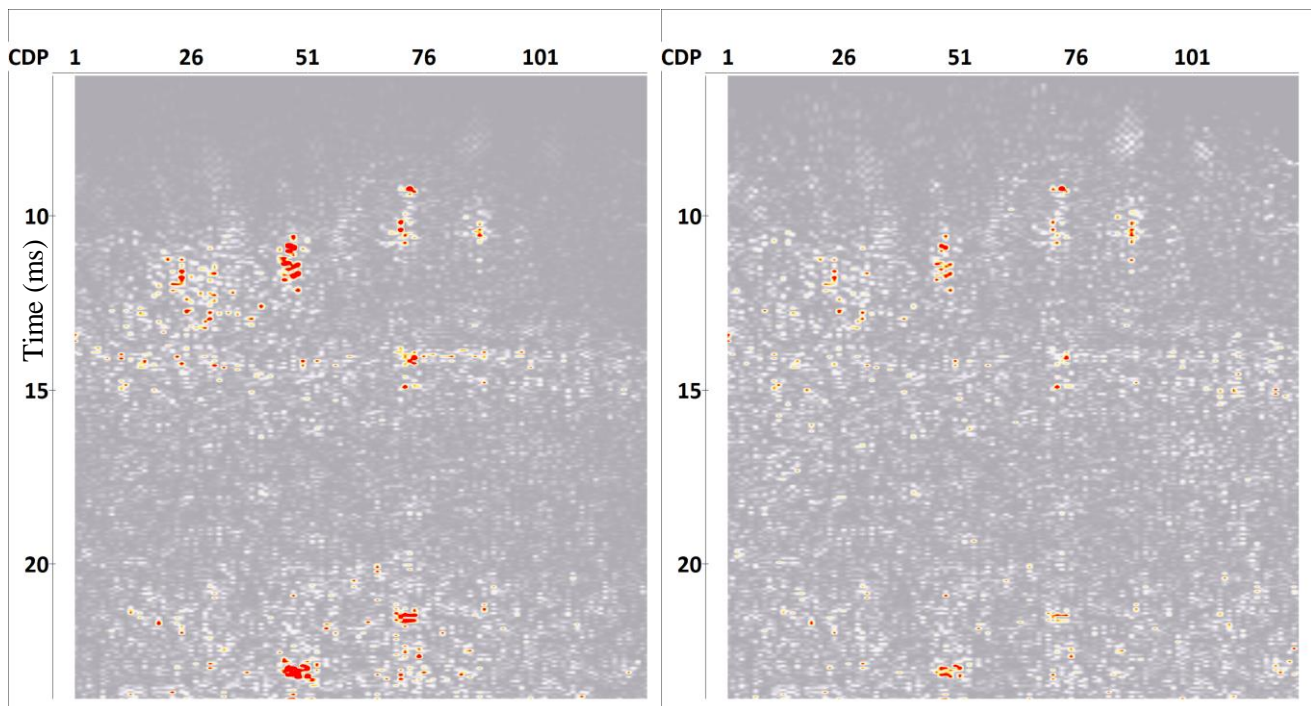
$$S(x_0, t_0) = \frac{1 \sum_{\delta t} \{ \sum_{i=1}^n D(x_i, t_k(x_i)) \}^2}{n \sum_{\delta t} \{ \sum_{i=1}^n D^2(x_i, t_k(x_i)) \}}$$

Here, D is the diffracted wavefield, x and t are the space and time coordinates, and t_k are the diffraction traveltimes. We can see that the semblance is a result of diffraction wavefield summation along diffraction traveltimes curves (which is basically migration) squared and divided by the result of migration of the square of the diffracted wavefield. One can observe that the semblance can be approximated by the division of two migration results. The diffraction semblance is similar to the energy in a sense that it highlights the apexes of the diffractions, however it also provides a more even amplitude for the diffracted anomalies, as it measures the coherence of the diffracted wavefield along the traveltimes curve instead of simply measuring its energy. On the diffraction semblance attribute, diffractions have more even amplitudes.

We compute the semblance using the same [Pre/Post-Stack Kirchhoff Time Migration*](#) module. The computed result will not be strictly equal to the semblance due to the presence of migration weights in [Pre/Post-Stack Kirchhoff Time Migration*](#), which are absent from the equation above. Still, the

resulting attribute provides useful additional information.

In the flow **005-semblance**, we first compute the square of the diffracted wavefield with **Power of Trace** and migrate it using the **Pre/Post-Stack Kirchhoff Time Migration*** - this gives the denominator of the above semblance definition. After this, we take the previously computed diffraction energy (which is precisely the squared migration result in the numerator of the semblance definition) and divide it by the migrated square of the diffracted wavefield with the **Trace Math** module. This results in the semblance image shown in the Figure below, which still highlights the diffractions, but has a more even amplitude distribution compared to diffraction energy and can be used in some cases for detection of weaker diffractions. It also suppresses the remaining reflections, which could be present in a diffraction energy image.



Diffraction energy (left) compared to diffraction semblance (right)

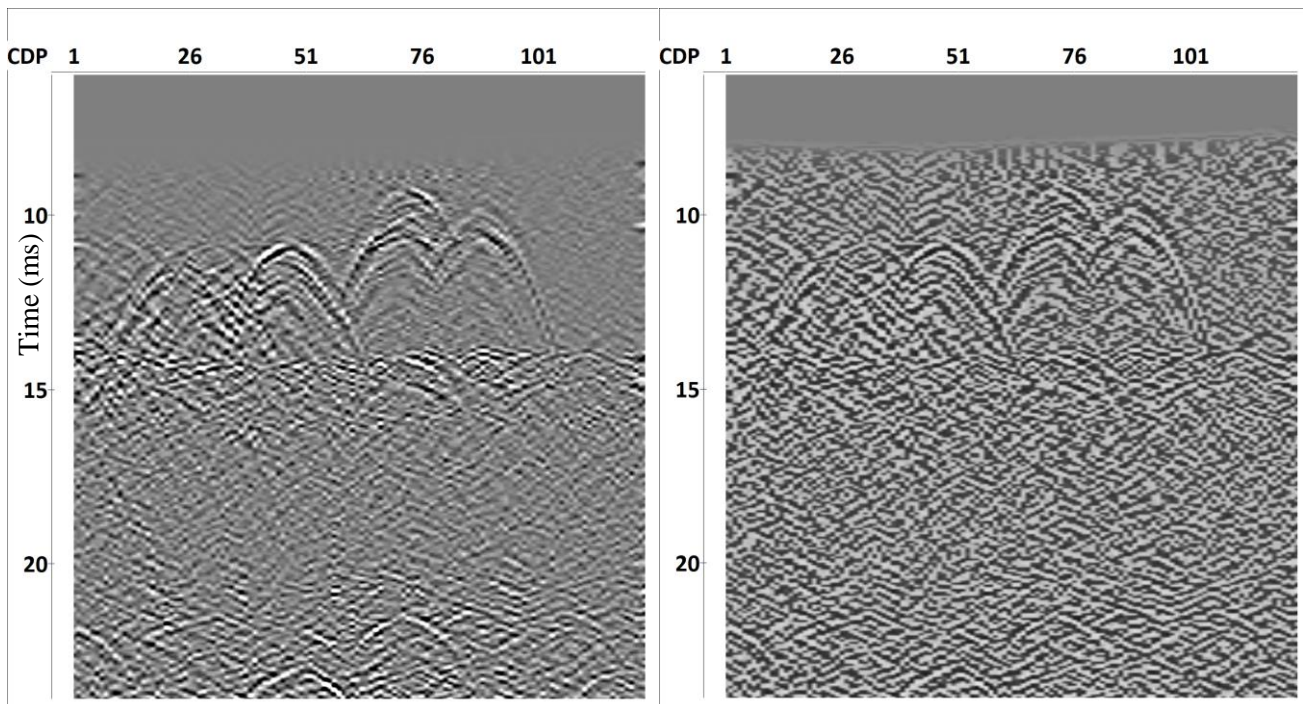
N-th root migration

In the flow **006-nth-root-migration**, we apply another method for detection of weak diffractions, which is the migration of the N-th root wavefield (Rost and Thomas, 2002). This method suggests computing the N-th root of the diffracted wavefield, followed by a migration. The N-th root of the wavefield is computed as follows:

$$\sqrt[n]{D(x, t)} = \text{sgn}(D(x, t)) \sqrt[n]{|D(x, t)|}$$

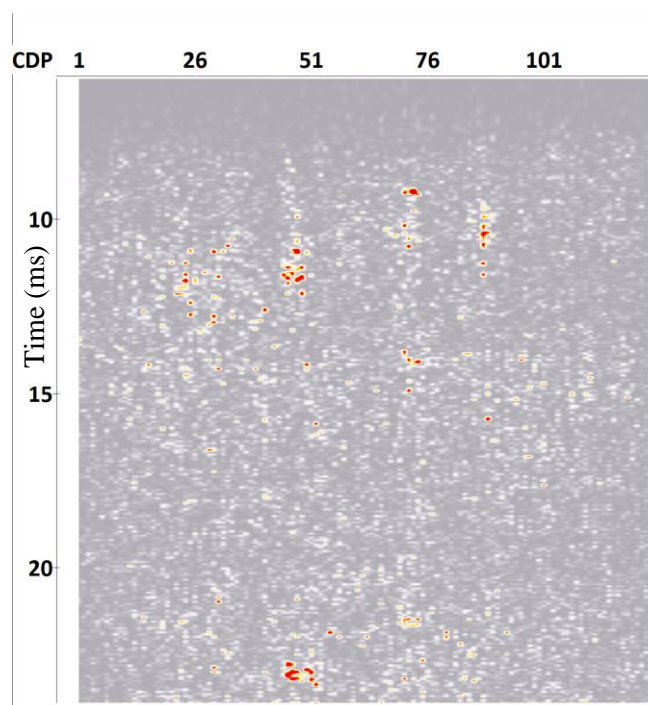
The N-th root operation artificially reduces the dynamic range of the data, raising the relative amplitude of the originally low-amplitude diffraction tails, thus making the migration more focused on the tails instead of apices and remaining reflections. To compute the N-th root, we simply use the **Power of Trace** module in the 'Keep sign' mode and the *Power exponent* less than 1 (we use 0.2 in the tutorial

project, which is equivalent to the 5th root of the wavefield).



Diffracted wavefield before (left) and after (right) 5th root computation

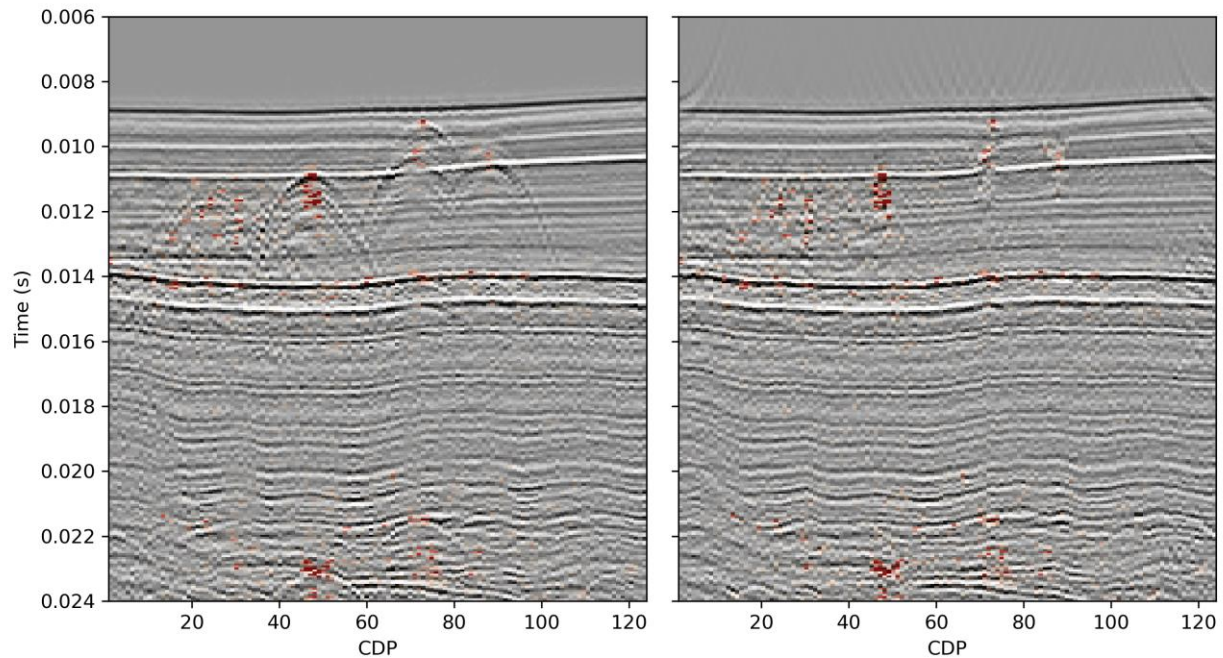
After this, we apply the same steps which were previously applied to the separated diffracted wavefield to obtain the diffraction energy shown below. One can observe that N-th root wavefield also helps to highlight the weaker diffractions and suppress the remaining reflection energy.



Diffraction energy computed from the 5th root wavefield

One can also compute the semblance from the N-th root wavefield similar to how it was computed in the previous section.

One can observe that the amplitude maxima on the diffraction attributes from this tutorial correspond to the true locations of the heterogeneities which cause the diffractions. This can be demonstrated by overlaying one of these attributes over the original and migrated seismic images (the overlay was done outside of **RadExPro**). This makes the attributes useful for the studies of small-scale heterogeneities and risk assessment.



Diffraction energy overlayed over original (left) and migrated (right) seismic data.

References

- Decker, L., Merzlikin, D., & Fomel, S. (2017). Diffraction imaging and time-migration velocity analysis using oriented velocity continuation. *Geophysics*, 82(2), U25-U35.
- Denisov M.S. (2017). Seismic migration as a tool for true amplitude depth imaging of small objects. *Seismic technology*, 4, 51–72. (in Russian)
- Fomel, S. (2002). Applications of plane-wave destruction filters. *Geophysics*, 67(6), 1946-1960.
- Rost, S., & Thomas, C. (2002). Array seismology: Methods and applications. *Reviews of geophysics*, 40(3), 2-1.
- Schwarz, B. (2019). An introduction to seismic diffraction. In *Advances in geophysics* (Vol. 60, pp. 1-64). Elsevier.